Development 137, 2753-2762 (2010) doi:10.1242/dev.049627

The activation of membrane targeted CaMK-II in the zebrafish Kupffer's vesicle is required for left-right asymmetry

Ludmila Francescatto, Sarah C. Rothschild, Alexandra L. Myers and Robert M. Tombes*

SUMMARY

Intracellular calcium ion (Ca^{2+}) elevation on the left side of the mouse embryonic node or zebrafish Kupffer's vesicle (KV) is the earliest asymmetric molecular event that is functionally linked to lateral organ placement in these species. In this study, Ca^{2+}/CaM-dependent protein kinase (CaMK-II) is identified as a necessary target of this Ca^{2+} elevation in zebrafish embryos. CaMK-II is transiently activated in approximately four interconnected cells along the anterior left wall of the KV between the six- and 12-somite stages, which is coincident with known left-sided Ca^{2+} elevations. Within these cells, activated CaMK-II is observed at the surface and in clusters, which appear at the base of some KV cilia. Although seven genes encode catalytically active CaMK-II in early zebrafish embryos, one of these genes also encodes a truncated inactive variant (αKAP) that can hetero-oligomerize with and target active enzyme to membranes. αKAP, β2 CaMK-II and γ1 CaMK-II antisense morpholino oligonucleotides, as well as KV-targeted dominant negative CaMK-II, randomize organ laterality and *southpaw* (*spaw*) expression in lateral plate mesoderm (LPM). Left-sided CaMK-II activation was most dependent on an intact KV, the PKD2 Ca^{2+} channel and γ1 CaMK-II; however, αKAP, β2 CaMK-II and the RyR3 ryanodine receptor were also necessary for full CaMK-II activation. This is the first report to identify a direct Ca^{2+}-sensitive target in left-right asymmetry and supports a model in which membrane targeted CaMK-II hetero-oligomers in nodal cells transduce the left-sided PKD2-dependent Ca^{2+} signals to the LPM.

KEY WORDS: CaMK-II (Camk2), Calcium, Asymmetry, Nodal, Kupffer's vesicle, Cilia

INTRODUCTION

Laterality disorders are characterized by the misplacement of one or more organs across the left-right (LR) axis and occur as often as once in every 6000 newborns (Peeters and Devriendt, 2006). Although the positioning of internal organs in diverse vertebrate organisms is initiated by signals originating from a transient posterior structure, known as the mouse embryonic node or zebrafish Kupffer's vesicle (KV), this pathway remains incompletely defined (Hirokawa et al., 2006).

The KV is a fluid-filled organ that forms at the posterior end of the notochord at the early somite stages of teleosts (Essner et al., 2005). The KV, like the mouse ventral node, is lined by epithelial cells that contain motile cilia whose resultant fluid flow is necessary to establish left-right asymmetry (Kramer-Zucker et al., 2005; Lee and Anderson, 2008). Fluid flow leads to the asymmetric expression of *southpaw* (*spaw*) in left-sided lateral plate mesoderm (LPM) beginning at the 10- to 12-somite stage (Long et al., 2003). Southpaw, which is a member of the transforming growth factor (TGF) β family of secreted morphogens, is also expressed bilaterally in cells surrounding the KV at the four- to six-somite stage (Gourronc et al., 2007; Long et al., 2003). Expression of *nodal*, the mouse ortholog of *spaw*, also occurs both bilaterally in cells surrounding the ventral node and then later in left LPM (Yamamoto et al., 2003). Southpaw induces the progressive expression of additional *spaw*, *pitx2, lefty1* and *lefty2* in LPM (Long et al., 2003) that proceeds towards the anterior end of the embryo at a rate of approximately two somites per hour (Wang and Yost, 2008). This property of Southpaw/Nodal supports the reaction-diffusion model of self-induction (Shiratori and Hamada, 2006).

Ca^{2+} flux through the TRP channel PKD2 (polycystin 2) (Bisgrove et al., 2005; Schottenfeld et al., 2007) has been implicated in the undefined pathway that transfers signals from perinodal cells to the LPM (Langenbacher and Chen, 2008). In fact, the involvement of PKD2 and of both motile and sensory cilia (two-cilia model) prompted the proposal that left-sided Ca^{2+} elevation was an early asymmetric event (Tabin and Vogan, 2003). Sustained Ca^{2+} elevations were subsequently detected on the left side of the embryonic node in mice (McGrath et al., 2003; Tanaka et al., 2005), chick (Garic-Stankovic et al., 2008; Raya et al., 2004) and zebrafish at the five- to eight-somite stage (Jurynec et al., 2008; Sarmah et al., 2005). In addition to PKD2, left-sided Ca^{2+} release has been linked to ryanodine receptors (Garic-Stankovic et al., 2008; Jurynec et al., 2008) and inositol phosphate-dependent signals (Sarmah et al., 2005), implicating intracellular Ca^{2+} amplification. Gap junctions may enable Ca^{2+} to spread through target cells on the left side of the node (Hatler et al., 2009; Levin and Mercola, 1999) and H^+K^+ATPase may help maintain the driving force for Ca^{2+} elevations (Garic-Stankovic et al., 2008). PKD2 targeted to endomembranes in KV cells may be more important than plasma membrane PKD2 for left-right asymmetry in zebrafish (Fu et al., 2008). The importance of PKD2 is further supported by observations that *pkd2* morphants and mutants randomize organ placement and LPM *spaw* (Bisgrove et al., 2005; Schottenfeld et al., 2007). PKD2-deficient mouse embryos also lack the normal Ca^{2+} elevation on the left side of the ventral node (McGrath et al., 2003) and have randomized organ position (McGrath et al., 2003; Pennekamp et al., 2002).

Department of Biology, Virginia Commonwealth University, Richmond, VA 23284-2012, USA

*Author for correspondence (rtombes@vcu.edu)

Accepted 12 June 2010

The target of the nodal Ca^{2+} elevation has remained elusive. Any candidate Ca^{2+}-sensing molecule must be activated simultaneously with Ca^{2+} elevations but prior to LPM *spaw* expression. Although PK-C, calcineurin and CaM (calmodulin) kinases are developmentally expressed Ca^{2+}-sensing molecules with potential roles in transducing signals generated at the node (Whitaker, 2006), none of these molecules has been implicated as targets of the asymmetric Ca^{2+} signal. CaMK-II, the type II multifunctional Ca^{2+}/CaM-dependent protein kinase is the most widely expressed member of the CaM kinase family (Tombes et al., 2003) and is subject to highly orchestrated stimulatory and inhibitory autophosphorylations, which then influence its subcellular location and activity towards a variety of substrates (Colbran, 2004; Griffith, 2004; Swulius and Waxham, 2008). Seven transcriptionally active genes encoding CaMK-II have been described in early zebrafish embryos, with one gene containing two open reading frames (Rothschild et al., 2009; Rothschild et al., 2007). During development, CaMK-II is best known for its role in non-canonical Wnt-dependent convergent extension and planar cell polarity (PCP) pathways (Kühl et al., 2000; Sheldahl et al., 2003).

In this study, we report that endogenous zebrafish CaMK-II is transiently activated in cells comprising the left wall of the KV at the same time that left-sided Ca^{2+} elevations are known to occur. The subcellular localization of activated CaMK-II is consistent with the nature of the genes encoding CaMK-II that are implicated in asymmetry and suggests a means by which CaMK-II laterally transduces Ca^{2+} signals from the KV to left LPM.

MATERIALS AND METHODS

Zebrafish strains

Wild-type zebrafish embryos (AB and WIK Strains) were obtained through natural matings, raised at 28.5°C in the presence of 0.002% Methylene Blue and 0.003% PTU (1-phenyl-2-thiourea) to block pigmentation, and staged as described (Kimmel et al., 1995). Embryos were injected at the one- to four-cell stage with ~1 nl using freshly pulled micropipettes attached to a precision pressurized injector (Kimmel et al., 1995).

CaMK-II antibodies

Immunolocalization using anti-phosphorylated (Thr^{287}) CaMK-II has previously been described by this laboratory (Easley et al., 2006). All zebrafish CaMK-II proteins have a sequence of MHRQE[pT^{287}]VECLK in this region (Rothschild et al., 2009; Rothschild et al., 2007), which is very similar to the phosphopeptide antigen used to create this rabbit polyclonal antibody (MHRQE[pT]VDCLK; Upstate/Millipore) and are therefore predicted to crossreact. E^{289} is the only (conservative) difference in the epitope. This well-characterized antibody has been shown to be dependent on autophosphorylated (P-Thr^{287}) mammalian CaMK-II (Rich and Schulman, 1998). An additional pan-specific CaMK-II antibody (total CaMK-II) was also used in this study (BD Biosciences). Although this antibody was reactive with all ectopically expressed zebrafish CaMK-IIs tested by immunoblot so far, including αKAP, $\delta 1_G$ and $\beta 1_K$, it could not detect total CaMK-II in whole mount embryos until ~24 hpf.

Autophosphorylation, immunoblot and CaMK-II autonomy assays

To test the reactivity of the anti-P-T^{287} antibody with zebrafish CaMK-II, a cDNA encoding full-length zebrafish $\beta 1_K$ CaMK-II (Rothschild et al., 2007) was amplified by RT-PCR from 48 hpf zebrafish heart cDNA and inserted in-frame with the FLAG-GFP N-terminal epitope in the pCDNA vector (Seward et al., 2008) and transfected into mouse cells using Lipofectamine 2000 (Invitrogen). After 24 hours, ~50 μg of cell lysate, prepared in EGTA as described, was autophosphorylated for various lengths of time (5 seconds to 5 minutes) on ice in the presence or absence of Ca^{2+} and CaM (Rich and Schulman, 1998; Tombes et al., 1995). The majority of each sample was then prepared in SDS buffer for immunoblot; 20 μg was probed with the anti-P-T^{287} antibody (10 μg/ml) and 5 μg with the total CaMK-II antibody (1 μg/ml). The remainder was simultaneously diluted into EGTA and then assayed for Ca^{2+}/CaM-independent activity (autonomy) by measuring the percentage of autocamtide-2 phosphorylation in the presence of Ca^{2+}/CaM that persists in the absence of Ca^{2+}/CaM (Rothschild et al., 2007).

Immunolocalization

Fresh embryos were fixed in 4% paraformaldehyde in PBS and stored in methanol. Embryos were sequentially incubated with rabbit anti-P-Thr^{287} CaMK-II IgG, goat anti-rabbit $Alexa^{568}$ (Invitrogen) as described (Easley et al., 2006); and with mouse anti-acetylated α tubulin IgG (Sigma) and goat anti-mouse $Alexa^{488}$ (Invitrogen). Whole-mount immunoreactivity with the P-Thr^{287} antibody was non-existent when only secondary antibodies were used and was undetectable anywhere else in the embryo at the somite stage. Embryos were confocally imaged (Nikon C1 Plus) on a Nikon E-600 compound microscope using 20, 40 or 100× objectives. The number of cells that exhibited activated CaMK-II and their location was determined from inspections of *z*-stacks of up to 40 0.5-1.0 μm optical sections. The percentage of embryos that expressed any active CaMK-II was scored and the total number of cells per embryo was averaged for all embryos, including those that had no activation. In some cases, *z*-stacks were converted into projections that merged optical sections into one image.

Morpholinos

Morpholino antisense oligonucleotides (MOs) were designed to disrupt translation by complementarity to predicted or known translational start sites of zebrafish CaMK-II cDNAs. MOs were purchased from Gene Tools (Philomath OR) and are shown for each gene in the 5′ to 3′ direction with the sequence corresponding to the start codon underlined and mRNA nucleotide positions indicated. The *camk2b1* and *camk2b2* MOs have previously been described and optimized (Rothschild et al., 2009). The control mismatch MO exhibits 13 (*camk2aKAP*), 16 (*camk2b2*) and 15 (*camk2g1*) nucleotide mismatches on the corresponding mRNA.

camk2a: GCCATCCTGGAAGCGTGTGCGCCTC-3′; nucleotides –20 to +5

camk2aKAP: GGCATAGCGGTGGTCTGCTCTCCAC; nucleotides –20 to +5

camk2b1: GGCCATGTCTTCCCGTCTCGGACTC; nucleotides –19 to +6

camk2b2: GCGTGCAGGTTGTGGTTGCCATGTC; nucleotides –3 to +19)

camk2g1: AATTGTAGCCATGTTGTGTGTGCGT; nucleotides –13 to +12)

camk2g2: AATTGTAGCCATGTTGCGCTTTACG; nucleotides –13 to +12)

camk2d1: CAGGTTGTTGAAGCCATGCTGAAAG; nucleotides –8 to +17)

camk2d2: CAGATGGTCAGAGCCATTGTGATG; nucleotides –7 to +17)

Mismatch: CAATGCTCACAGCGATTGTCATG

Morpholino stocks (1 mM) were stored at –80°C. Prior to injection, MO aliquots were heated to 65°C for 5 minutes, cooled to room temperature and then diluted in Danieau buffer (Westerfield, 1993). The dose-dependent effectiveness of each MO at suppressing CaMK-II expression was assessed by CaMK-II peptide assay, as described previously (Rothschild et al., 2009; Rothschild et al., 2007). The zebrafish *pkd2* MO (5′-AGGACGA-ACGCGACTGGAGCTCATC-3′), previously described to phenocopy *pkd2* mutants (Schottenfeld et al., 2007; Sun et al., 2004), the *ryr3* MO (Jurynec et al., 2008) and the *no tail* (*ntl*) MO (Amack et al., 2007) were all injected at 4 ng.

Whole-mount in situ hybridization, RT-PCR, probes and cDNA clones

Embryos were fixed and hybridized with ~0.5 kb digoxigenin-labeled antisense riboprobes and then developed as previously described (Rothschild et al., 2009). The zebrafish *cmlc2* (cardiac myosin light chain 2) probe was previously described (Rothschild et al., 2009). The *foxa3* probe was prepared from a cDNA provided by Dr J. A. Lister; the *southpaw, charon* and *lefty1* probes from clones provided by Dr H. J. Yost;

and the *ntl* probe was from Dr D. M. Garrity. The *camk2aKAP* probe contains ~100 bp of unique sequence that encodes the membrane-targeting domain; the remainder of its coding sequence is shared with *camk2a* catalytic mRNAs. The *camk2aKAP* probe was prepared from a clone (Open Biosystems) using a *camk2aKAP* sense primer similar to the *camk2aKAP* MO and a *camk2a* antisense primer. The same *camk2aKAP* splice variant was identified by sequencing over 15 TOPO/TA clones that had amplified from embryonic mRNA at the four- to eight-cell stage (maternal), 14- to 18-somite stage and 2 dpf dissected cardiac tissue. The *camk2g1* probe was synthesized from a partial zebrafish ($\gamma 1_C$ variant) cDNA clone in the TOPO/TA vector, which had been amplified by RT-PCR (Rothschild et al., 2007). The *camk2b2* probe was synthesized from a partial cDNA clone spanning the variable domain and corresponding to the $\beta 2_G$ variant, as previously described (Rothschild et al., 2009). The *sox17*-CaMK-II $K^{43}A$ construct was prepared by linking the 4.2 kb upstream sequence of the zebrafish *sox17* gene (Chung and Stainier, 2008) to human GFP-CaMK-II (Rothschild et al., 2009). Site-specific ($K^{43}A$) mutagenesis and enzymatic inactivation were confirmed by sequencing and CaMK-II assays.

Analysis of KV cilia

Live embryos were imaged using differential interference contrast optics after transient anesthesia with 0.003% Tricaine (MS222, Sigma) and immobilization between coverslips. Ciliary motility was imaged in the Kupffer's vesicle of live anesthetized embryos using a NIKON 60× water immersion Plan APO objective with DIC optics and 30 frames per second acquisitions. Lengths of cilia in fixed embryos were determined from anti-acetylated α-tubulin wholemounts using quantitative length algorithms in Nikon Elements in three to four experimental replicates for at least ten embryos per replicate and ~20 cilia per embryo. Statistical analyses were performed using the paired *t*-test. Statistically significant differences are denoted by an asterisk and indicated *P*-values.

RESULTS

CaMK-II is activated in cells on the left side of the Kupffer's vesicle

Although left-sided Ca^{2+} elevations occur between the five- and eight-somite stage in cells surrounding the KV (Jurynec et al., 2008; Sarmah et al., 2005), the subsequent signaling event has remained undetermined. In this study, CaMK-II was evaluated as a potential Ca^{2+} target at the KV. In zebrafish embryos, CaMK-II expression accelerates around the segmentation period, appearing in a wide variety of tissues (Rothschild et al., 2009; Rothschild et al., 2007). Upon activation by Ca^{2+}/CaM, CaMK-II autophosphorylates at Thr^{287} to sustain its own activity (Hudmon and Schulman, 2002a). Immunolocalization of P-Thr^{287} CaMK-II can therefore be used to identify cells in which natural relevant Ca^{2+} signals activated CaMK-II. This well-characterized antibody (Rich and Schulman, 1998) has previously been used to localize activated CaMK-II in tissues as diverse as mammalian neurons (Easley et al., 2006) and *Xenopus* embryos (Kühl et al., 2000).

Activated (P-Thr^{287}) CaMK-II was detected in ciliated cells lining the left side of the KV (Fig. 1A,B). Activated CaMK-II was undetectable in the developing embryo prior to KV formation, which is not surprising as CaMK-II expression is minimal until ~10 hpf (Rothschild et al., 2007). Later, CaMK-II is activated in some, but not all, of the other embryonic locations where expression has been observed (Rothschild et al., 2007), such as the forebrain (data not shown). Within cells surrounding the KV, activated CaMK-II is enriched at cell surfaces (arrow) and in clusters (arrowhead), which sometimes occur at the base of cilia (Fig. 1C-E). Punctate and cortical staining of endogenous activated CaMK-II is reminiscent of CaMK-II clustering previously reported in kidney cells and neurons (Hudmon et al., 2005).

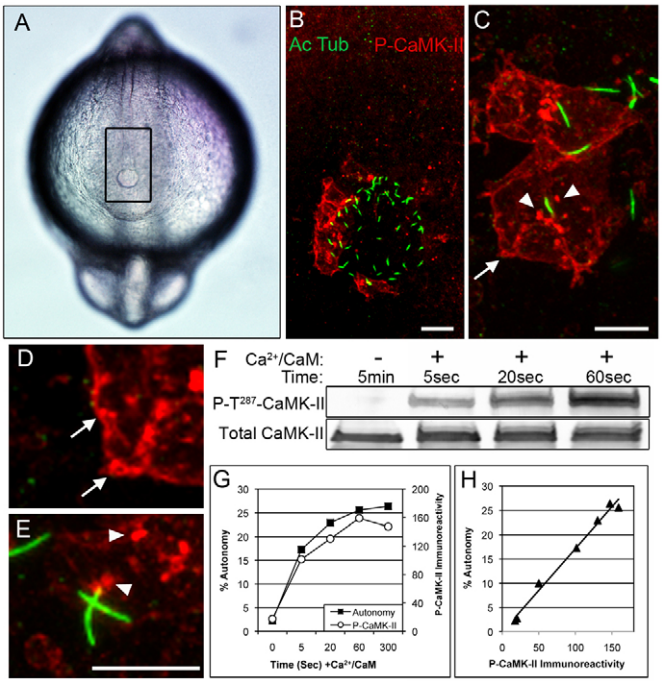

Fig. 1. CaMK-II is activated on the left side of Kupffer's vesicle (KV). (**A**) Dorsal view of a 12-somite embryo, shows the KV (at the bottom of outlined rectangle) by differential interference contrast microscopy. (**B**) Confocal immunofluorescence of rectangular region in A using anti-acetylated α-tubulin (green, Alexa 488) to localize cilia and anti-P-T^{287} CaMK-II (red, Alexa 568) to localize activated CaMK-II in cells on the left side of the KV. (**C-E**) Higher magnification reveals activated CaMK-II along the cell cortex (arrows) and intracellular clusters (arrowheads), which occasionally colocalize with the base of cilia. Scale bars 10 μm. (**F-H**) The anti-P-T^{287} antibody reacts only with activated CaMK-II, as demonstrated by incubating ectopically expressed zebrafish $\beta 1_K$ CaMK-II with Ca^{2+}/CaM for the indicated times and then assessing (F) immunoreactivity with anti-P-T^{287} CaMK-II and an antibody reactive with total CaMK-II. (G) CaMK-II autonomy, measured by peptide assay, and P-T^{287} immunoreactivity for a representative experiment. (H) When values from four experimental replicates were compiled and plotted against each other, P-T^{287} CaMK-II immunoreactivity (blot density) was proportional to autonomy.

The anti-P-Thr^{287} antibody was predicted to react with zebrafish CaMK-IIs, as the sequence surrounding this important regulatory region is highly conserved (Tombes et al., 2003). This was confirmed using cloned and autophosphorylated zebrafish CaMK-II (Fig. 1F). As Thr^{287} autophosphorylation renders CaMK-II active in the absence of Ca^{2+}, the proportionality of such Ca^{2+}-independent activity (autonomy; Fig. 1G) to P-Thr^{287} immunoreactivity is demonstrated (Fig. 1H), as previously shown for mammalian CaMK-II (Rich and Schulman, 1998). Although the total CaMK-II antibody reacts with overexpressed zebrafish CaMK-II (Fig. 1F), it could not detect endogenous CaMK-II in wholemounts prior to 24 hpf (data not shown).

Left-sided CaMK-II activation is transient

Activated CaMK-II was not detected at the KV until the three- to six-somite stage when it became weakly apparent bilaterally (Fig. 2A,B). As development proceeded, activated CaMK-II increased in intensity primarily, but not exclusively, in cells on the left side of the KV at 10 (Fig. 2C) and 12 somites (Fig. 1). The number of cells that

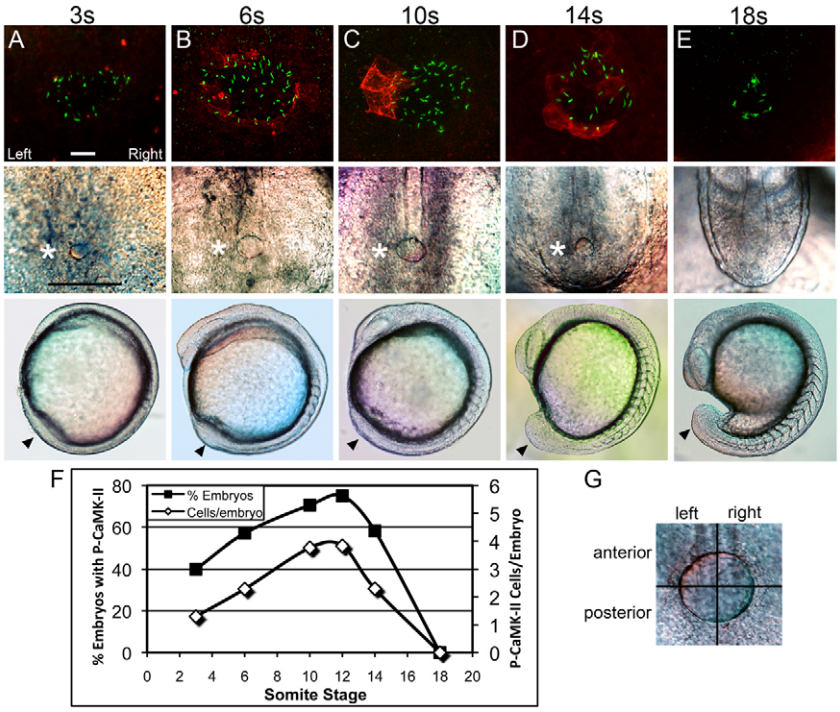

Fig. 2. Left-sided CaMK-II activation is transient. (**A-E**) The top row shows representative confocal immunofluorescent projections of P-T^{287} CaMK-II (red) and cilia (green) at the three- (A), six- (B), 10- (C), 14- (D) and 18- (E) somite stages. These projections of *z*-stacks were conducted as in Fig. 1 (12 somites) and are displayed at the same intensity. Scale bar: 10 μm. Middle row shows KV morphology (asterisk) from the same dorsal perspective. Scale bar: 100 μm. Bottom row shows the position of the KV (arrowheads) from the lateral perspective. (**F**) For each stage (*n*=14-36 embryos per stage), the percentage of embryos and the number of cells per embryo that exhibited activated CaMK-II was determined by inspecting *z*-stacks. (**G**) The location of KV cells exhibiting activated CaMK-II was scored in one of the four quadrants shown here and results can be found in Tables 1 and 2.

exhibited activated CaMK-II and their location was determined from inspections of *z*-stacks of each embryo (see Movies 1 and 2 in the supplementary material). The number of embryos and cells per embryo expressing activated CaMK-II peaked at the 10- to 12-somite stage (Fig. 2F). As many as ten, but on average four, cells contained activated CaMK-II and were almost always in contact with each other, spanning the height of the KV, occasionally including cells at the base, but never on the roof. The proportion of active cells that were anterior and left-sided also peaked between 10 and 12 somites (Table 1). At any one of these peak times, no more than 75% of embryos exhibited P-CaMK-II. It is possible that the other 25% of embryos had already peaked and inactivated CaMK-II. After this stage, CaMK-II rapidly inactivated and was completely lost in all embryos by 18 somites around the disassembling KV (Fig. 2F,G). Activated CaMK-II was not observed in cells outside of the immediate vicinity of the KV, in the notochord or along lateral plate mesoderm, indicating that any role for CaMK-II in propagating the asymmetry signal is restricted to cells lining the functional KV.

CaMK-II suppression randomizes left-right organ placement

Both gene-specific antisense morpholino oligonucleotides (MOs) and a dominant-negative CaMK-II construct were used to assess the functional necessity of CaMK-II activity in the determination of left-right asymmetry. Of the seven genes encoding zebrafish CaMK-II (α1, β1, β2, γ1, γ2, δ1, δ2), translation-blocking MOs that target two of these genes (β1, β2) have already been described (Rothschild et al., 2009). As one gene (α1) uses two promoters to yield catalytically active (α1) and inactive (αKAP) products, a total of eight unique MOs were evaluated. Three of these MOs, as well as kinase inactive (K^{43}A) GFP-CaMK-II (Fig. 3A), targeted using the *Sox17* promoter (Chung and Stainier, 2008), interfered with organ placement. *Sox17* is known to be expressed in dorsal forerunner cells (DFC) and in cells lining the KV (Amack et al., 2007). As previously shown (Amack et al., 2007), the Sox17 promoter targeted K^{43}A CaMK-II to DFCs at the shield stage and to cells surrounding the KV at the 12-somite stage (Fig. 3A). K^{43}A CaMK-II is not gene specific, as it can hetero-oligomerize with any endogenous CaMK-II and decrease inter-subunit autophosphorylation (Johnson et al., 2000). Targeted K^{43}A CaMK-II induced fewer defects than did CaMK-II MOs, which is consistent with an endodermal/KV-specific role for CaMK-II in asymmetry, in addition to its many other developmental roles.

The three effective MOs (*camk2b2, camk2aKAP, camk2g1*) disrupted the normal asymmetry of heart, brain and visceral organs at low (1-2 ng) MO levels when compared with a control mismatch MO (Fig. 3B). Organ laterality was assessed by heart jogging at 24 hpf (*cmlc2*), visceral organ positioning at 48hpf (*foxa3*) and dorsal diencephalon or epithalamus (*lefty1*) asymmetry at the 22- to 26-somite stage (Fig. 3C). None of the other MOs interfered with left-

Table 1. The presence and location of activated CaMK-II at various somite stages

Somite stage	Embryos (*n*)	% embryos with P-T^{287}	Number of cells/embryo with P-T^{287}	% P-T^{287} cells on left	% P-T^{287} cells anterior
3	15	40	1.3	55	45
6	14	57	2.3	72	56
10	17	71	3.8	73	66
12	36	75	3.8	84	68
14	36	58	2.3	68	24
18	15	0	0.0	–	–

The percentage of embryos exhibiting activated KV CaMK-II (P-T^{287}), the average number of activated cells per embryo and their position at the indicated somite stages are given.

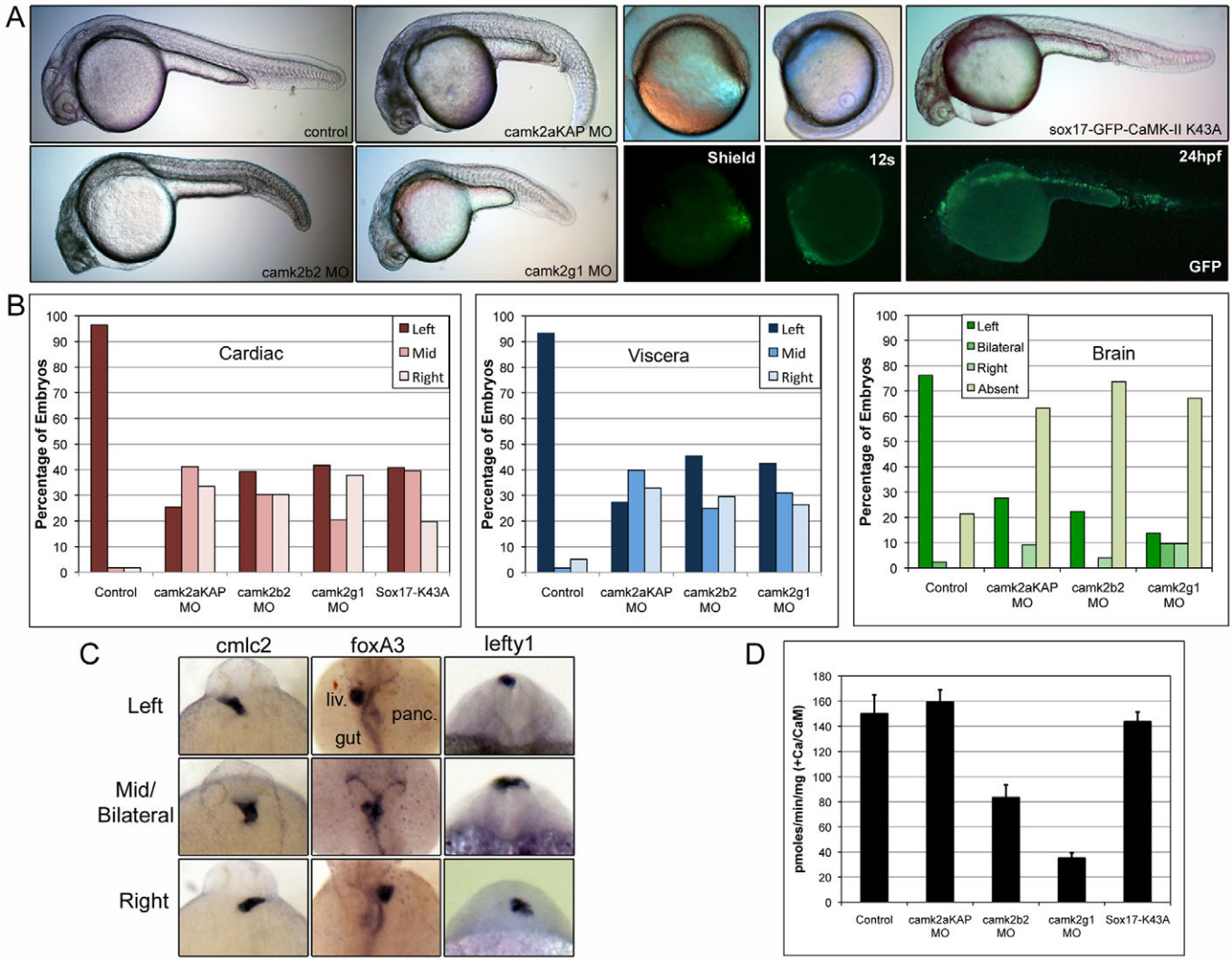

Fig. 3. Left-right asymmetry is lost in CaMK-II morphants. (**A**) Lateral images of representative morphant embryos at 24 hpf and of Sox17-$K^{43}A$ GFP CaMK-II cDNA-injected embryos at shield stage, 12 somites and 24 hpf include fluorescent (GFP) images. (**B**) Organ asymmetry was scored for embryos injected with 5 ng mismatch, 1.5 ng *camk2aKAP*, 1.5 ng *camk2b2*, 1.25 ng *camk2g1* MOs and 150 pg Sox17-GFP-CaMK-II $K^{43}A$ cDNA; *n*=87-233 per condition. (**C**) Representative dorsal views of *camk2g1* morphant embryos stained with probes for *cmlc2* (cardiac, 24 hpf), *foxa3* (visceral organ, 48 hpf) and *lefty1* (epithalamus, ~24 somites). (**D**) Ca^{2+}/CaM-dependent CaMK-II activity in pmoles/minute/mg were determined by peptide assays on 24 hpf lysates after injection with the indicated MO or cDNA.

right asymmetry at up to 5 ng, as shown for the mismatch MO (Fig. 3B). Targeted kinase-inactive CaMK-II (Sox17-$K^{43}A$) also randomized heart laterality (Fig. 3B). Visceral organ development was disrupted by Sox17-$K^{43}A$ to the extent that laterality could not be determined. Unlike *cmlc2* and *foxa3*, *lefty1* was absent from the epithalamus (but not the notochord) in 60-70% of all three *camk2* morphants. The absence of epithalamic *lefty1* expression has also been reported in *pkd2* morphants (Bisgrove et al., 2005), suggesting Ca^{2+}-dependent *lefty1* brain expression.

camk2g1 and *camk2b2* MOs decreased total embryonic CaMK-II levels at 24 hpf, whereas the *camk2aKAP* MO and the Sox17-$K^{43}A$ cDNA construct had no effect, as expected (Fig. 3D). Although *camk2a*, *camk2b1* and *camk2g2* MOs also suppressed activity during the first 3 days of development to varying degrees (data not shown) (Rothschild et al., 2009), they had no effect on organ laterality. These findings are consistent with the involvement of specific CaMK-II-encoding genes in organ asymmetry.

Zebrafish αKAP structure

No previous report has implicated αKAP in non-muscle function. The alternative promoter responsible for αKAP expression is found 3′ to catalytic domain exons (Bayer et al., 1998; Tombes et al., 2003). As translation begins downstream from the exon encoding Thr^{287} (Fig. 4A), αKAP cannot be directly detected with the anti P-Thr^{287} antibody. However, truncated constructs such as αKAP efficiently hetero-oligomerize with full-length CaMK-IIs (Lantsman and Tombes, 2005) to anchor active complexes in cell membranes (Bayer et al., 1998). The sequence of the first 29 residues of αKAP is shown (Fig. 4B), ending at the corresponding lysine $(K)^{317}$ in full-length α CaMK-II (Rothschild et al., 2007). The zebrafish αKAP sequence is homologous to mouse αKAP (Fig. 4B) and both sequences are predicted to be membrane spanning (Bendtsen et al., 2004). RT-PCR of zebrafish αKAP during the first 2 days of development identified only the non-nuclear variant, not the reported nuclear-targeted αKAP variant (O'Leary et al., 2006).

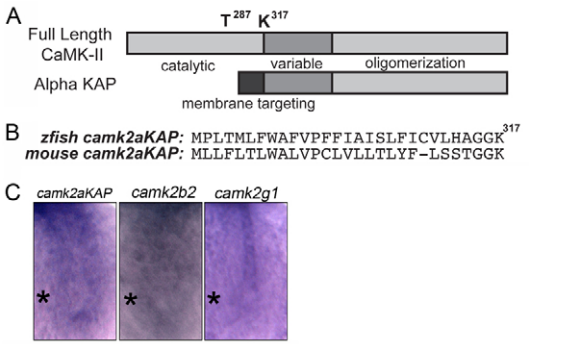

Fig. 4. CaMK-II mRNAs are uniformly detected around the KV. (**A**) αKAP encodes an alternative membrane-targeting domain. (**B**) Mouse and zebrafish αKAP sequences. (**C**) Dorsal view of *camk2aKAP*, *camk2b2* and *camk2g1* in situ hybridization at 12 somites. Asterisk indicates KV location.

CaMK-IIs are uniformly expressed around the KV

CaMK-II mRNA distribution was assessed in order to rule out asymmetric expression of CaMK-II-encoding genes. This was the only feasible approach as CaMK-II protein levels were below the detection limits of the total CaMK-II antibody at this early stage. *camk2aKAP*, *camk2b2* and *camk2g1* mRNAs were all expressed around the KV at the 10- to 12-somite stage (Fig. 4C). *camk2aKAP* and *camk2b2* were expressed in cells surrounding the KV and the notochord, whereas *camk2g1* was more enriched in cells within the notochord. With all three genes, expression was uniformly bilateral, thus indicating no preferential left-sided expression of any CaMK-II.

KV morphology and function in CaMK-II morphants

In order to determine whether the roles of these three CaMK-II-encoding genes could be explained by alterations in the morphology, structure or function of the notochord, KV or cilia, morphants around the 10-somite stage (Fig. 5A, lateral) were evaluated. Morphants exhibited no delays in notochord and KV formation or gene expression as shown dorsally (Fig. 5A, dorsal) and by in situ hybridization of *ntl* (Fig. 5A, ntl) and the KV-specific marker *charon* (Fig. 5A, charon). The stereotypical horseshoe expression pattern of *charon* (Hashimoto et al., 2004) was unaffected in morphants, although the breadth of *charon* expression was contracted, as were the KVs themselves. The distribution of cilia throughout the KV appeared relatively normal (Fig. 5A, cilia), but their number was decreased by ~25% in *camk2b2* and *camk2g1* morphants, whereas their length (measured upon magnification as in Fig. 1E) was decreased by 35-40% (Fig. 5B). Ciliary number and length was decreased by only 10-20% in *camk2aKAP* morphants, even though their asymmetry defects were no less severe than *camk2b2* or *camk2g1* morphants. KV ciliary beating appeared unaffected in all morphants (see Movies 3-6 in the supplementary material). These findings indicate that the loss of asymmetry was not the result of severe morphogenic deficiencies in the KV or cilia.

Expression of laterality markers downstream from CaMK-II

The earliest known gene product in zebrafish embryos that exhibits left sidedness is *southpaw* (*spaw*), the ortholog of the TGFβ family member *nodal* (Wang and Yost, 2008). Left-sided CaMK-II

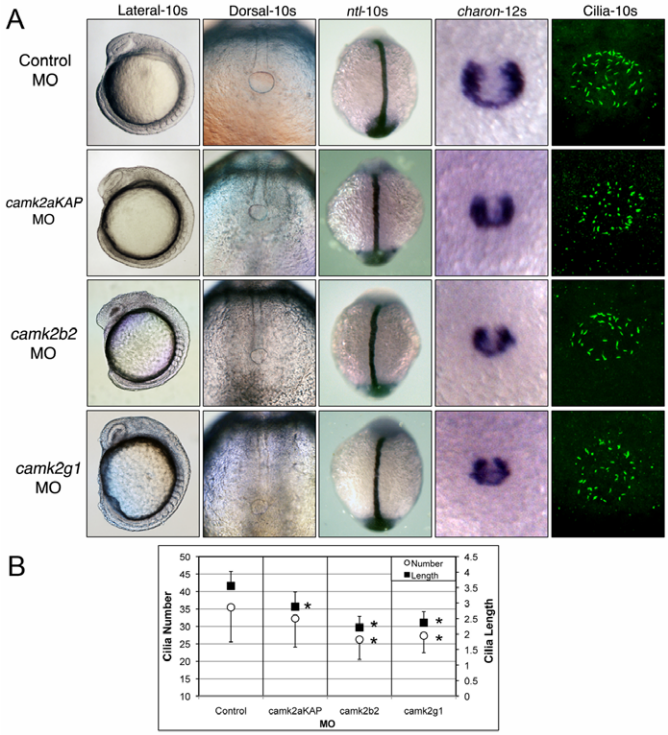

Fig. 5. KV markers and cilia in CaMK-II morphants. (**A**) Embryos were probed with *ntl* (10s), *charon* (12s) and anti-acetylated tubulin (Cilia-10s) after injection with 5 ng mismatch (control), 1.5 ng *camk2aKAP*, 1.5 ng *camk2b2* or 1.25 ng *camk2g1* MO. (**B**) Cilia number and length were averaged from 105-201 embryos per condition; **P*<0.005 compared with control.

activation precedes the expression of *spaw* in left-sided LPM (Long et al., 2003). At 18-20 somites, 90-95% of control embryos exhibited *spaw* expression in left-sided LPM (Fig. 6). By contrast, *spaw* expression in all three CaMK-II morphants, as well as in Sox17-K^{43}A-injected embryos, was randomly distributed in LPM on the left, right or both sides. Although as many as 20% of morphant embryos exhibited an absence of LPM *spaw* expression; these findings indicate that the LPM *spaw* expression pathway was generally intact and that its sidedness had been randomized. At the KV, bilateral *spaw* expression was not disrupted in any morphant (data not shown), thus supporting the preferential influence of

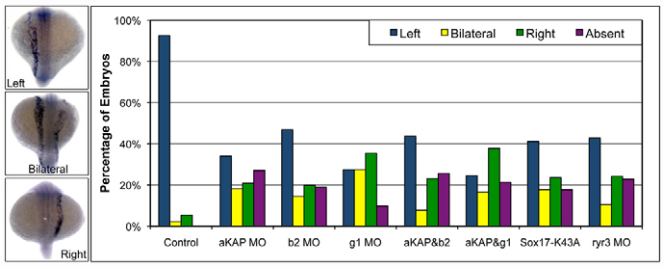

Fig. 6. *Spaw* asymmetry is lost. Left, bilateral, right or absent *spaw* expression was examined by in situ hybridization (as shown in samples) in single and double morphants of *camk2aKAP*, *camk2b2*, *camk2g1*, *ryr3* and sox17-K^{43}A CaMK-II at 18-20 somites and is listed as the percentage of the total embryos in each condition; *n*=39-145. Control embryos include mismatch MO-injected and buffer-injected embryos.

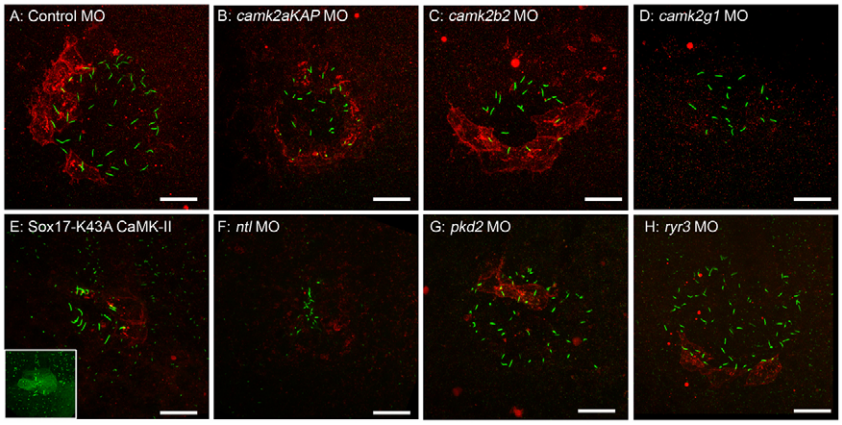

Fig. 7. CaMK-II activation is disrupted in morphants. Confocal immunofluorescent projections of P-T^{287} CaMK-II (red) and cilia (green) in embryos at the 12-somite stage after injection with (**A**) 5 ng mismatch (control), (**B**) 1.5 ng *camk2aKAP*, (**C**) 1.5 ng *camk2b2*, (**D**) 1.25 ng *camk2g1* MO, (**E**) 150 ng Sox17-K^{43}A GFP-CaMK-II cDNA (inset is green fluorescence of cilia and GFP-CaMK-II around the KV), (**F**) 4 ng *ntl* MO, (**G**) 4 ng *pkd2* MO or (**H**) 4 ng *ryr3* MO. Scale bar: 10 μm.

CaMK-II on *spaw* expression in LPM. Previous studies have shown that left-sided Ca^{2+} elevations are also dependent on the RyR3 ryanodine receptor (Jurynec et al., 2008); however, no studies have demonstrated its influence on left right asymmetry. We report that *ryr3* morphants have randomized cardiac and visceral organ asymmetry (see Fig. S1 in the supplementary material) and randomized *spaw* (Fig. 6).

The co-injection of wild type CaMK-II efficiently reverses the effects of *camk2b2* MOs on heart looping and morphogenesis (Rothschild et al., 2009). However, neither universally nor KV-targeted wild-type or constitutively active CaMK-II cDNA co-injections rescued laterality defects in *camk2g1* or *camk2aKAP* morphants, perhaps because such rescues would require left-sided expression of membrane-targeted CaMK-II to the KV. Widespread expression using the β-actin promoter, of low levels (~50 pg) of zebrafish αKAP or K^{43}A, but not wild-type CaMK-II cDNA (Rothschild et al., 2009) caused axis defects, presumably by inappropriate membrane targeting or inactivation of endogenous CaMK-II in other tissues (data not shown).

Morphant effects on KV CaMK-II

Our findings predict that activated CaMK-II in morphants should either be diminished or displaced. We found that KV CaMK-II activation was altered in embryos in which CaMK-II synthesis or activity was suppressed by MOs or dominant-negative CaMK-II (Fig. 7, Table 2). *camk2aKAP* morphants showed an overall reduction in activated CaMK-II, primarily owing to preferential loss of cortical CaMK-II (Fig. 7B). Activated CaMK-II levels were not diminished in *camk2b2* morphants and the protein was still present in most embryos, but was located more bilaterally and more posteriorly (Fig. 7C). The most profound reduction was in *camk2g1* morphants (Fig. 7D) where fewer than one-third of embryos exhibited activated CaMK-II and, on average, fewer than one activated cell was present per embryo. Embryos injected with Sox17-K^{43}A CaMK-II also showed a reduction of KV CaMK-II activation (Fig. 7E), with simultaneous GFP expression in ciliated KV cells (Fig. 7E inset). These results are consistent with γ1 CaMK-II-αKAP hetero-oligomers comprising the sensory CaMK-II in cells surrounding the KV, while β2 CaMK-II may influence a subtle aspect of KV assembly, stability or function.

Morphants that disrupt KV formation and suppress Ca^{2+} channel expression also interfered with CaMK-II activation. *ntl* morphants have a contracted distorted nonfunctional KV (Amack et al., 2007) that completely lacks any activated CaMK-II (Fig. 7F). *pkd2* morphants have asymmetry defects (Bisgrove et al., 2005; Schottenfeld et al., 2007) and also exhibit a substantial reduction in P-Thr^{287} CaMK-II (Fig. 7G), even though total embryonic CaMK-II expression was not altered in these morphants at 24 hpf or 72 hpf (as determined by CaMK-II peptide assay, data not shown). *ryr3* morphants also exhibited diminished numbers of cells containing activated CaMK-II (Fig. 7H, Table 2).

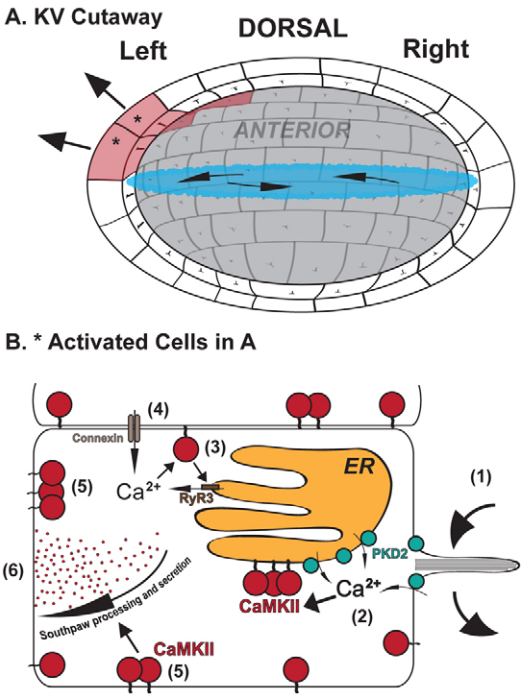

Fig. 8. Model of CaMK-II activation in the KV. (**A**) The KV is shown from a posterior cutaway view to demonstrate counterclockwise fluid flow over ciliated cells. Four anterior interconnected cells are shown with activated CaMK-II (pink) on the left wall of the KV. (**B**) Adjacent activated cells on the left side of the KV (from A) show a sequence of (1) activation of cilia by fluid flow or morphogen binding, (2) PKD2-dependent Ca^{2+} release via cilia and ER, (3) activation of membrane targeted hetero-oligomers of αKAP and γ1 CaMK-II to activate further Ca^{2+} release via ryanodine receptors (RyR3), (4) Ca^{2+} diffusion to adjacent cells via gap junctions (connexin), and (5) clustering of activated CaMK-II to induce (6) *southpaw* processing or secretion.

Table 2. The presence and location of activated CaMK-II in different morphants

Morphant	Embryos (*n*)	% embryos with P-T^{287}	Number of cells/embryo with P-T^{287}	% P-T^{287} cells on left	% P-T^{287} cells anterior
Control	36	75	3.8	84	68
camk2aKAP MO	19	21	2.0	47	33
camk2b2 MO	20	80	3.4	44	44
camk2g1 MO	21	29	0.9	25	10
sox17-K^{43}A CaMK-II	18	33	1.9	57	61
ntl MO	33	0	0.0	0	0
pkd2 MO	21	43	1.3	60	48
ryr3 MO	43	58	2.4	48	34

The percentage of embryos exhibiting activated KV CaMK-II, the number of cells per embryo and their position in different morphants are given.

DISCUSSION

In this study, the Ca^{2+}/CaM-dependent protein kinase, CaMK-II, is identified as an essential Ca^{2+}-sensitive molecule that is responsible for left-right asymmetry in zebrafish. This conclusion is based on observations that the transient activation of CaMK-II in cells on the left side of KV is necessary for normal organ laterality. Based on known structural and functional features of CaMK-II, our findings implicate products of three CaMK-II-encoding genes and two Ca^{2+} channels into a model through which CaMK-II action links KV function with LPM signaling.

CaMK-II is a KV sensory molecule

CaMK-II is the likely direct target of the Ca^{2+} elevations known to occur on the left side of the zebrafish KV. Nodal Ca^{2+} elevations are dependent on both PKD2 (McGrath et al., 2003) and the RyR3 ryanodine receptor (Jurynec et al., 2008). In this study, we have demonstrated that KV CaMK-II activation is also dependent on PKD2 and RyR3. CaMK-II also presents itself as a link between these two channels as it is known to directly phosphorylate and promote RyR channel opening (Zalk et al., 2007).

The requirement for multiple CaMK-II gene products is not surprising as CaMK-IIs naturally form hetero-oligomers. In fact, αKAP is only known to act as a hetero-oligomer by targeting active β CaMK-II to the sarcoplasmic reticulum membrane (Nori et al., 2003; Singh et al., 2005). In addition to directly phosphorylating the RyR Ca^{2+} channel (Zalk et al., 2007), SR CaMK-II is also believed to promote excitation-contraction coupling by phosphorylating phospholamban, a protein that is necessary for activating SERCA, the Ca^{2+}ATPase (Maier and Bers, 2007). Our findings are consistent with this function in embryonic hearts as αKAP morphants show a 30% decrease in heart rates, even at 2 dpf (data not shown).

In non-muscle tissue, αKAP presumably still targets CaMK-II to membrane sites necessary to respond to relevant Ca^{2+} elevations within the cell. This is supported by the loss of cortical KV CaMK-II in αKAP morphants. The γ1 and β2 CaMK-II splice variants known to be expressed at this time are relatively simple, lacking known targeting domains of their own (Rothschild et al., 2009; Rothschild et al., 2007) and would therefore be influenced by hetero-oligomerization with αKAP. Our studies suggest that hetero-oligomers of αKAP with γ CaMK-II are necessary for transducing the Ca^{2+} signal released by the KV. It is less likely that β CaMK-II is the sensory CaMK-II, as *camk2b2* morphants did not diminish CaMK-II activation in cells around the KV. Although activated CaMK-II was not observed in KV cilia, α, γ and δ CaMK-IIs have all been reported in the ciliary/centrosome proteome database (Gherman et al., 2006).

CaMK-II is now the earliest Ca^{2+}-dependent molecular marker shown to exhibit left-sidedness in zebrafish. Its peak activation occurs between 10 and 12 somites, does not persist past 16 somites and is dependent on KV assembly, as demonstrated using *ntl* morphants. Activated CaMK-II does not appear in the LPM or notochord, so its function must remain local. CaMK-II morphants do not affect perinodal *spaw* transcription, but do influence distant (LPM) *spaw* expression, which begins around the 12-somite stage (Wang and Yost, 2008). The involvement of activated CaMK-II in linking KV asymmetry to LPM is compatible with either the two cilia (physical) or the morphogen gradient (chemical) model (Hirokawa et al., 2006).

Model of action

Based on these and other findings, a model of KV CaMK-II action can be considered (Fig. 8). Ca^{2+} elevations in left sided cells of the KV occur between the five- and eight-somite stage (Jurynec et al., 2008; Sarmah et al., 2005) as a result of morphogen binding or fluid flow sensation. Ca^{2+} elevations necessary to activate CaMK-II require PKD2 (TRPP2) acting through extracellular influx and/or endomembrane release (Fu et al., 2008), and the additional activation of intracellular Ca^{2+} release pathways involving the ryanodine receptor, Ryr3 (Jurynec et al., 2008). By the 8- to 10-somite stage, αKAP-γ1 CaMK-II hetero-oligomers are preferentially activated in approximately four interconnected left anterior KV cells. This pattern of activation suggests a role for gap junctions, which is supported by evidence that the gap junction protein connexin, Cx43.4, is necessary for left-right asymmetry and contributes to KV morphogenesis (Hatler et al., 2009). Similar to a subset of CaMK-II, connexin 43.4 is expressed in puncta within cells surrounding the KV (Hatler et al., 2009). Activated CaMK-II is enriched at such clusters, which are found throughout cells, including at the base of cilia. CaMK-II clusters have previously been observed in other cell types and are dependent on autophosphorylation (Hudmon et al., 2005). CaMK-II activation begins to diminish after the 12-somite stage, at which time *spaw* mRNA begins to appear in LPM. Our evidence suggests that for any individual embryo, peak CaMK-II activation at the KV can occur anytime between 6 and 12 somites, and then rapidly disappears.

It has been postulated that preferential left-sided processing, secretion or transport of Southpaw/Nodal from the embryonic node to the left LPM is the most likely, and perhaps simplest, mechanism linking Ca^{2+}-dependent events in perinodal cells to the LPM (Shiratori and Hamada, 2006). One possible means by which CaMK-II could influence this pathway is through its known effect on protein secretion via proteins, such as synapsin (Easom, 1999; Herrmann et al., 2005; Nayak et al., 1996). Synapsin I is a known substrate of CaMK-II (Nayak et al., 1996) and is present in the trans-Golgi network of epithelial cells (Bustos et al., 2001). Alternatively, left-sided CaMK-II could enhance left-sided Southpaw action through the degradation of the Southpaw antagonist Charon (Hashimoto et al., 2004). In the absence of

biased Ca^{2+} signals, slower but constitutive bilateral synthesis, secretion or function of Southpaw would lead to bilateral or random LPM activation.

CaMK-II is a morphogenic molecule

Our results are also consistent with a role for CaMK-II in the morphogenesis of the KV. Although we have not detected activated CaMK-II immunologically in embryos prior to the somite stage, CaMK-II mRNAs and activity have been detected during shield and epiboly stages (Rothschild et al., 2007). During these early stages, Ca^{2+} signals mediated by the Na^{+}/Ca^{2+} transporter (NCX4a) have been shown to be essential for KV morphogenesis (Shu et al., 2007). Our findings indicate that CaMK-II influences KV cilia length and numbers, but unlike NCX4a, CaMK-II is not absolutely required for KV formation or for ciliary motility. These results suggest that the persistence of the KV may actually depend on CaMK-II activation; as Ca^{2+} transients in the KV subside, the inactivation of CaMK-II may lead to KV disassembly. KV morphology defects are more prominent in *camk2b2* and *camk2g1* morphants than in *camk2aKAP* morphants, suggesting a non-membrane role for CaMK-II in ciliary stability. The presence of activated CaMK-II clusters at the base of cilia is consistent with their role in the stability and thus the length of cilia. In fact, the length of cilia in PKD2 morphants is known to be similarly decreased by ~40% (Bisgrove et al., 2005), suggesting that PKD2 is sufficient to supply the Ca^{2+} signals that activate CaMK-II to influence ciliary stability. CaMK-II could also contribute to KV morphogenesis through steps that involve cell migration (Amack et al., 2007) as CaMK-II is known to promote embryonic cell migration in culture (Easley et al., 2008) and non-canonical Wnt-dependent pathways that activate CaMK-II promote convergent extension cell migrations (Kühl et al., 2001).

Summary

The findings presented here provide insight into a longstanding mystery of a direct protein target of the Ca^{2+} elevation that is known to transduce signals from the KV to lateral plate mesoderm. The substrates of CaMK-II at the KV remain to be determined, but the importance of membrane-targeted hetero-oligomers of CaMK-II suggests relevant targets at the plasma membrane or at organelles. We propose that these targets promote translation, disinhibition and/or secretion of molecules that ultimately lead to left-sided Southpaw activation. Whether other Ca^{2+} targets exist and whether CaMK-II is the left-sided Ca^{2+} target at the embryonic node in other species awaits further analysis. CaMK-IIs also influence KV ciliagenesis and are expressed at many other times and places during zebrafish development (Rothschild et al., 2009; Rothschild et al., 2007). CaMK-II is emerging as even more multi-functional than previously envisioned (Hudmon and Schulman, 2002b), supporting its universal ability to decode a wide variety of Ca^{2+} signals. This study has established a valuable approach to define the relative intracellular activity level and location of catalytically active members of this ubiquitous enzyme during development.

Acknowledgements

The authors gratefully acknowledge Jamie J. McLeod, Bennett S. Childs, Carolyn Conway and Amritha Yelamilli for their assistance with this study, and Rebecca Burdine, Marnie Halpern, James Lister, Amanda Dickinson, Debbie Garrity and Joe Yost for sharing useful reagents and advice. Supported by National Science Foundation grant IOS-0817658.

Competing interests statement

The authors declare no competing financial interests.

Supplementary material

Supplementary material for this article is available at
http://dev.biologists.org/lookup/suppl/doi:10.1242/dev.049627/-/DC1

References

Amack, J. D., Wang, X. and Yost, H. J. (2007). Two T-box genes play independent and cooperative roles to regulate morphogenesis of ciliated Kupffer's vesicle in zebrafish. *Dev. Biol.* **310**, 196-210.

Bayer, K. U., Harbers, K. and Schulman, H. (1998). AlphaKAP is an anchoring protein for a novel CaM kinase II isoform in skeletal muscle. *EMBO J.* **17**, 5598-5605.

Bendtsen, J. D., Nielsen, H., von Heijne, G. and Brunak, S. (2004). Improved prediction of signal peptides: SignalP 3.0. *J. Mol. Biol.* **340**, 783-795.

Bisgrove, B. W., Snarr, B. S., Emrazian, A. and Yost, H. J. (2005). Polaris and Polycystin-2 in dorsal forerunner cells and Kupffer's vesicle are required for specification of the zebrafish left-right axis. *Dev. Biol.* **287**, 274-288.

Bustos, R., Kolen, E. R., Braiterman, L., Baines, A. J., Gorelick, F. S. and Hubbard, A. L. (2001). Synapsin I is expressed in epithelial cells: localization to a unique trans-Golgi compartment. *J. Cell Sci.* **114**, 3695-3704.

Chung, W. S. and Stainier, D. Y. (2008). Intra-endodermal interactions are required for pancreatic beta cell induction. *Dev. Cell* **14**, 582-593.

Colbran, R. J. (2004). Targeting of calcium/calmodulin-dependent protein kinase II. *Biochem. J.* **378**, 1-16.

Easley, C. A., Faison, M. O., Kirsch, T. L., Lee, J. A., Seward, M. E. and Tombes, R. M. (2006). Laminin activates CaMK-II to stabilize nascent embryonic axons. *Brain Res.* **1092**, 59-68.

Easley, C. A., Brown, C. M., Horwitz, A. F. and Tombes, R. M. (2008). CaMK-II promotes focal adhesion turnover and cell motility by inducing tyrosine dephosphorylation of FAK and paxillin. *Cell Motil. Cytoskeleton* **65**, 662-674.

Easom, R. A. (1999). CaM kinase II: a protein kinase with extraordinary talents germane to insulin exocytosis. *Diabetes* **48**, 675-684.

Essner, J. J., Amack, J. D., Nyholm, M. K., Harris, E. B. and Yost, H. J. (2005). Kupffer's vesicle is a ciliated organ of asymmetry in the zebrafish embryo that initiates left-right development of the brain, heart and gut. *Development* **132**, 1247-1260.

Fu, X., Wang, Y., Schetle, N., Gao, H., Putz, M., von Gersdorff, G., Walz, G. and Kramer-Zucker, A. G. (2008). The subcellular localization of TRPP2 modulates its function. *J. Am. Soc. Nephrol.* **19**, 1342-1351.

Garic-Stankovic, A., Hernandez, M., Flentke, G. R., Zile, M. H. and Smith, S. M. (2008). A ryanodine receptor-dependent Ca(i)(2+) asymmetry at Hensen's node mediates avian lateral identity. *Development* **135**, 3271-3280.

Gherman, A., Davis, E. E. and Katsanis, N. (2006). The ciliary proteome database: an integrated community resource for the genetic and functional dissection of cilia. *Nat. Genet.* **38**, 961-962.

Gourronc, F., Ahmad, N., Nedza, N., Eggleston, T. and Rebagliati, M. (2007). Nodal activity around Kupffer's vesicle depends on the T-box transcription factors Notail and Spadetail and on Notch signaling. *Dev. Dyn.* **236**, 2131-2146.

Griffith, L. C. (2004). Regulation of calcium/calmodulin-dependent protein kinase II activation by intramolecular and intermolecular interactions. *J. Neurosci.* **24**, 8394-8398.

Hashimoto, H., Rebagliati, M., Ahmad, N., Muraoka, O., Kurokawa, T., Hibi, M. and Suzuki, T. (2004). The Cerberus/Dan-family protein Charon is a negative regulator of Nodal signaling during left-right patterning in zebrafish. *Development* **131**, 1741-1753.

Hatler, J. M., Essner, J. J. and Johnson, R. G. (2009). A gap junction connexin is required in the vertebrate left-right organizer. *Dev. Biol.* **336**, 183-191.

Herrmann, T. L., Morita, C. T., Lee, K. and Kusner, D. J. (2005). Calmodulin kinase II regulates the maturation and antigen presentation of human dendritic cells. *J. Leukocyte Biol.* **78**, 1397-1407.

Hirokawa, N., Tanaka, Y., Okada, Y. and Takeda, S. (2006). Nodal flow and the generation of left-right asymmetry. *Cell* **125**, 33-45.

Hudmon, A. and Schulman, H. (2002a). Neuronal Ca^{2+}/Calmodulin-dependent protein kinase II: the role of structure and autoregulation in cellular function. *Annu. Rev. Biochem.* **71**, 473-510.

Hudmon, A. and Schulman, H. (2002b). Structure-function of the multifunctional Ca^{2+}/calmodulin-dependent protein kinase II. *Biochem. J.* **364**, 593-611.

Hudmon, A., Lebel, E., Roy, H., Sik, A., Schulman, H., Waxham, M. N. and De Koninck, P. (2005). A mechanism for Ca^{2+}/calmodulin-dependent protein kinase II clustering at synaptic and nonsynaptic sites based on self-association. *J. Neurosci.* **25**, 6971-6983.

Johnson, L. D., Willoughby, C. A., Burke, S. H., Paik, D. S., Jenkins, K. J. and Tombes, R. M. (2000). δ Ca^{2+}/Calmodulin-dependent protein kinase II isozyme-specific induction of neurite outgrowth in P19 embryonal carcinoma cells. *J. Neurochem.* **75**, 2380-2391.

Jurynec, M. J., Xia, R., Mackrill, J. J., Gunther, D., Crawford, T., Flanigan, K. M., Abramson, J. J., Howard, M. T. and Grunwald, D. J. (2008). Selenoprotein N is required for ryanodine receptor calcium release channel

activity in human and zebrafish muscle. *Proc. Natl. Acad. Sci. USA* **105**, 12485-12490.
Kimmel, C. B., Ballard, W. W., Kimmel, S. R., Ullmann, B. and Schilling, T. F. (1995). Stages of embryonic development of the zebrafish. *Dev. Dyn.* **203**, 253-310.
Kramer-Zucker, A. G., Olale, F., Haycraft, C. J., Yoder, B. K., Schier, A. F. and Drummond, I. A. (2005). Cilia-driven fluid flow in the zebrafish pronephros, brain and Kupffer's vesicle is required for normal organogenesis. *Development* **132**, 1907-1921.
Kühl, M., Sheldahl, L., Malbon, C. C. and Moon, R. T. (2000). Ca^{2+}/Calmodulin-dependent protein kinase II is stimulated by Wnt and Frizzled homologs and promotes ventral cell fates in Xenopus. *J. Biol. Chem.* **275**, 12701-12711.
Kühl, M., Geis, K., Sheldahl, L. C., Pukrop, T., Moon, R. T. and Wedlich, D. (2001). Antagonistic regulation of convergent extension movements in Xenopus by Wnt/beta-catenin and Wnt/Ca^{2+} signaling. *Mech. Dev.* **106**, 61-76.
Langenbacher, A. and Chen, J. N. (2008). Calcium signaling: a common thread in vertebrate left-right axis development. *Dev. Dyn.* **237**, 3491-3496.
Lantsman, K. and Tombes, R. M. (2005). CaMK-II oligomerization potential determined using CFP/YFP FRET. *Biochim. Biophys. Acta* **1746**, 45-54.
Lee, J. D. and Anderson, K. V. (2008). Morphogenesis of the node and notochord: the cellular basis for the establishment and maintenance of left-right asymmetry in the mouse. *Dev. Dyn.* **237**, 3464-3476.
Levin, M. and Mercola, M. (1999). Gap junction-mediated transfer of left-right patterning signals in the early chick blastoderm is upstream of Shh asymmetry in the node. *Development* **126**, 4703-4714.
Long, S., Ahmad, N. and Rebagliati, M. (2003). The zebrafish nodal-related gene southpaw is required for visceral and diencephalic left-right asymmetry. *Development* **130**, 2303-2316.
Maier, L. S. and Bers, D. M. (2007). Role of Ca^{2+}/calmodulin-dependent protein kinase (CaMK) in excitation-contraction coupling in the heart. *Cardiovasc. Res.* **73**, 631-640.
McGrath, J., Somlo, S., Makova, S., Tian, X. and Brueckner, M. (2003). Two populations of node monocilia initiate left-right asymmetry in the mouse. *Cell* **114**, 61-73.
Nayak, A., Moore, C. and Browning, M. (1996). Ca^{2+}/calmodulin-dependent protein kinase II phosphorylation of the presynaptic protein synapsin I is persistently increased during long-term potentiation. *Proc. Natl. Acad. Sci. USA* **93**, 15451-15456.
Nori, A., Lin, P. J., Cassetti, A., Villa, A., Bayer, K. U. and Volpe, P. (2003). Targeting of alpha-kinase-anchoring protein (alpha KAP) to sarcoplasmic reticulum and nuclei of skeletal muscle. *Biochem. J.* **370**, 873-880.
O'Leary, H., Lasda, E. and Bayer, K. U. (2006). CaMKIIbeta association with the actin cytoskeleton is regulated by alternative splicing. *Mol. Biol. Cell* **17**, 4656-4665.
Peeters, H. and Devriendt, K. (2006). Human laterality disorders. *Eur. J. Med. Genet.* **49**, 349-362.
Pennekamp, P., Karcher, C., Fischer, A., Schweickert, A., Skryabin, B., Horst, J., Blum, M. and Dworniczak, B. (2002). The ion channel polycystin-2 is required for left-right axis determination in mice. *Curr. Biol.* **12**, 938-943.
Raya, A., Kawakami, Y., Rodriguez-Esteban, C., Ibanes, M., Rasskin-Gutman, D., Rodriguez-Leon, J., Buscher, D., Feijo, J. A. and Izpisua Belmonte, J. C. (2004). Notch activity acts as a sensor for extracellular calcium during vertebrate left-right determination. *Nature* **427**, 121-128.
Rich, R. C. and Schulman, H. (1998). Substrate-directed function of calmodulin in autophosphorylation of Ca^{2+}/calmodulin-dependent protein kinase II. *J. Biol. Chem.* **273**, 28424-28429.
Rothschild, S. C., Lister, J. A. and Tombes, R. M. (2007). Differential expression of CaMK-II genes during early zebrafish embryogenesis. *Dev. Dyn.* **236**, 295-305.
Rothschild, S. C., Easley, C. A., 4th, Francescatto, L., Lister, J. A., Garrity, D. M. and Tombes, R. M. (2009). Tbx5-mediated expression of Ca^{2+}/calmodulin-dependent protein kinase II is necessary for zebrafish cardiac and pectoral fin morphogenesis. *Dev. Biol.* **330**, 175-184.
Sarmah, B., Latimer, A. J., Appel, B. and Wente, S. R. (2005). Inositol polyphosphates regulate zebrafish left-right asymmetry. *Dev. Cell* **9**, 133-145.
Schottenfeld, J., Sullivan-Brown, J. and Burdine, R. D. (2007). Zebrafish curly up encodes a Pkd2 ortholog that restricts left-side-specific expression of southpaw. *Development* **134**, 1605-1615.
Seward, M. E., Easley, C. A., 4th, McLeod, J. J., Myers, A. L. and Tombes, R. M. (2008). Flightless-I, a gelsolin family member and transcriptional regulator, preferentially binds directly to activated cytosolic CaMK-II. *FEBS Lett.* **582**, 2489-2495.
Sheldahl, L. C., Slusarski, D. C., Pandur, P., Miller, J. R., Kühl, M. and Moon, R. T. (2003). Dishevelled activates Ca^{2+} flux, PKC, and CaMKII in vertebrate embryos. *J. Cell Biol.* **161**, 769-777.
Shiratori, H. and Hamada, H. (2006). The left-right axis in the mouse: from origin to morphology. *Development* **133**, 2095-2104.
Shu, X., Huang, J., Dong, Y., Choi, J., Langenbacher, A. and Chen, J. N. (2007). Na,K-ATPase alpha2 and Ncx4a regulate zebrafish left-right patterning. *Development* **134**, 1921-1930.
Singh, P., Leddy, J. J., Chatzis, G. J., Salih, M. and Tuana, B. S. (2005). Alternative splicing generates a CaM kinase II beta isoform in myocardium that targets the sarcoplasmic reticulum through a putative alphaKAP and regulates GAPDH. *Mol. Cell Biochem.* **270**, 215-221.
Sun, Z., Amsterdam, A., Pazour, G. J., Cole, D. G., Miller, M. S. and Hopkins, N. (2004). A genetic screen in zebrafish identifies cilia genes as a principal cause of cystic kidney. *Development* **131**, 4085-4093.
Swulius, M. T. and Waxham, M. N. (2008). Ca(2+)/Calmodulin-dependent protein kinases. *Cell. Mol. Life Sci.* **65**, 2637-2657.
Tabin, C. J. and Vogan, K. J. (2003). A two-cilia model for vertebrate left-right axis specification. *Genes Dev.* **17**, 1-6.
Tanaka, Y., Okada, Y. and Hirokawa, N. (2005). FGF-induced vesicular release of Sonic hedgehog and retinoic acid in leftward nodal flow is critical for left-right determination. *Nature* **435**, 172-177.
Tombes, R. M., Westin, E., Grant, S. and Krystal, G. (1995). G1 cell cycle arrest and apoptosis are induced in NIH 3T3 cells by KN-93, an inhibitor of CaMK-II (the multifunctional Ca^{2+}/CaM kinase). *Cell Growth Differ.* **6**, 1063-1070.
Tombes, R. M., Faison, M. O. and Turbeville, C. (2003). Organization and evolution of multifunctional Ca^{2+}/CaM-dependent protein kinase (CaMK-II) genes. *Gene* **322**, 17-31.
Wang, X. and Yost, H. J. (2008). Initiation and propagation of posterior to anterior (PA) waves in zebrafish left-right development. *Dev. Dyn.* **237**, 3640-3547.
Westerfield, M. (1993). *The Zebrafish Book: a Guide for The Laboratory use of Zebrafish (Brachydanio rerio)*. Eugene OR: University of Oregon Press.
Whitaker, M. (2006). Calcium at fertilization and in early development. *Physiol. Rev.* **86**, 25-88.
Yamamoto, M., Mine, N., Mochida, K., Sakai, Y., Saijoh, Y., Meno, C. and Hamada, H. (2003). Nodal signaling induces the midline barrier by activating Nodal expression in the lateral plate. *Development* **130**, 1795-1804.
Zalk, R., Lehnart, S. E. and Marks, A. R. (2007). Modulation of the ryanodine receptor and intracellular calcium. *Annu. Rev. Biochem.* **76**, 367-385.